Efficient solar heterogeneous photocatalytic degradation of metronidazole using heterojunction semiconductors hybrid nanocomposite, layered double hydroxides

Farid Aoudjit, Fouzia Touahra, Lamine Aoudjit, Ouiza Cherifi and Djamilla Halliche

ABSTRACT

This study focuses on the synthesis of various nanocomposites with heterojunction structures, MgAl-LDH (LDH = layered double hydroxides) hybrid with semiconductor such as MoO_3 and CuO. These solids were synthesized by co-precipitation method at constant pH and have been characterized extensively using atomic absorption spectroscopy (AAS), X-ray diffraction (XRD), Fourier transform infrared (FTIR) and transmission electron microscopy-energy dispersive X-ray (TEM-EDX) methods. The catalytic activity of nanocomposites was tested in the photocatalytic degradation under solar irradiation of emerging pollutants as the pharmaceutical metronidazole (MNZ). The experimental parameters, including initial MNZ concentration, the nature of oxide incorporate in the photocatalyst, catalyst loading were explored. All the synthesized samples showed high photocatalytic performances; the highest photocatalysis efficiency was achieved with the photocatalyst dose 1.5 g/L and initial MNZ concentration of 10 mg/L at neutral pH. The photocatalytic experimental results were fitted very well to the Langmuir-Hinshelwood model. From the obtained results the calcined LDH/semiconductors could be efficient for the photocatalytic process under solar irradiation of pharmaceuticals and may contribute in environmental remediation.

Key words | heterojunction, LDH, metronidazole, photocatalysis, removal, solar

Farid Aoudjit (corresponding author)
Ouiza Cherifi
Laboratory of Petrochemical Synthesis,
Faculty of Hydrocarbons and Chemistry,
University of M'Hamed Bougara,
Boumerdes 35000,
Algeria
E-mail: *faoudjit@yahoo.fr*

Farid Aoudjit
Process Engineering Department,
Universiy of Akli Mohand Oulhadj,
Bouira,
Algeria

Farid Aoudjit
Fouzia Touahra
Lamine Aoudjit
Ouiza Cherifi
Djamilla Halliche
Laboratory of Natural Gas Chemistry,
Faculty of Chemistry,
University of Sciences and Technology, Houari Boumediene,
Algiers 16 111,
Algeria

Fouzia Touahra
Centre de Recherche Scientifique et Technique en Analyses Physico-chimiques (CRAPC),
BP 384-Bou-Ismail-RP 42004, Tipaza,
Algeria

Lamine Aoudjit
Unité de Développement des équipements Solaires, UDES/Centre de Développement des Energies Renouvelables, CDER,
Bou Ismail, 42415, W. Tipaza,
Algeria

HIGHLIGHTS

- The hybrids of semiconductor (MoO3, CuO) and LDH improved OH radical generation and conducted to higher removal efficiency.
- The photocatalytic process using the renewable and inexpensive solar radiation was highly efficient for the removal of MNZ.
- Good rates of solar photodegradation were obtained.

INTRODUCTION

During the past few decades the consumption of pharmaceutical drugs was dramatically increased, which has increased their discharge into the environment. Several pharmaceuticals are detected in the environment originally from both human and veterinary use (Kanakaraju *et al.* 2018). The remediation of pharmaceuticals is not completely achieved; it has been reported that about 64% of emerging contaminants are only partially removed (50%), while up to 9% are not removed during their treatment (Pereira *et al.* 2019).

The application of a new process for removal of emerging contaminants from wastewaters has become necessary. In this context, the heterogeneous photocatalysis can be considered more promising for the removal of this kind of pollutants. The photocatalysis has attracted more attention nowadays, since it is considered low cost, environmentally friendly and efficient.

Recent reports have demonstrated the efficient methods as adsorption and photocatalytic degradation for the

doi: 10.2166/wst.2020.519

removal of pharmaceutical pollutions. Nguyen *et al.* have conducted a research involving the removal of acetaminophen using commercially activated carbon, their results demonstrated that the adsorption occurred rapidly, with around 52% of acetaminophen in solution (517 mg/L) being removed within 5 min of contact (Nguyen *et al.* 2020). Czech *et al.* studied the photocatalytic of metoprolol and triclosan onto elsmoreite/tungsten oxide@ZnS they observed degradation of 50% of metoprolol and 70% of triclosan after exposure time of about 60 min under visible light (Czech *et al.* 2020). Ahmadpour *et al.* demonstrate excellent photocatalytic efficiency of diclofenac onto TiO_2@$ZnFe_2O_4$/Pd; they obtained degradation efficiency of 86.1% within 120 min under solar light (Ahmadpour *et al.* 2020).

The activation of semiconductor by the solar light irradiation is considered as renewable and inexpensive energy sources (Fagan *et al.* 2016; Mecha *et al.* 2016). The semiconductors used as photocatalysts are ZnO (Zhang *et al.* 2017), TiO_2 (Pichat *et al.* 2005), Cds (He *et al.* 2012) and SnO_2 (Kim *et al.* 2016). This recent year's the use of layered double hydroxides (LDH) as photocatalysts attracted more attention due to their advantages such as high specific surface area, easily controllable interlayer anions, simple synthesis, ability to generate electron-hole carriers, low cost and stability. LDH, also known as hydrotalcite-like compounds, are a class of synthetic anionic layered clays containing brucite-like layers and positively-charged sheets. They can be represented by the general formula: $[M^{2+}_{1-x}M^{3+}_{x}(OH)_2]^{x+}.(A^{n-}_{x/n}).mH_2O$; where M^{2+} and M^{3+} are the divalent and trivalent cations, respectively, A^{n-} represents the interlayer anion with a charge (n-) and x is equal to the ratio of $M^{3+}/(M^{2+}+M^{3+})$ with a value varying in the range of 0.17–0.50 (Zhao *et al.* 2012).

Photocatalysis using hybrids of semiconductors and LDH get great attention, and could be the most privileged catalysts (Prasad *et al.* 2019) as they have unique features because of the coupling of the individual characteristics of the parent sample.

In this work, we report the obtained results of high efficiency removal of pharmaceutical pollutant by efficient and environment friendly solar photocatalytic degradation using the heterojunction semiconductors hybrid nanocomposite, LDH. The photocatalysts were prepared via a coprecipitation method and theirs structural and physicochemical proprieties were analyzed by several techniques. The photocatalytic removal behavior of MNZ on the synthesized semiconductor/LDH using solar irradiations is investigated as a function of photocatalyst dose, initial pollutant concentration and nature of oxide incorporated. The results showed that the 5%MoO_3/MgAl-LDH-C can significantly improve remediation of pharmaceuticals.

EXPERIMENTAL

Materials

Semiconductors photocatalysts synthesis

The MgAl-LDH materials were prepared by co-precipitation method at constant pH (10) with cationic ratio (Mg^{2+}/Al^{3+}) equal to 2. 100 mL of nitrate salts solution containing $Al(NO_3)_3{\cdot}9H_2O$ and $Mg(NO_3)_2{\cdot}6H_2O$ was added dropwise to an alkaline solution containing Na_2CO_3 and NaOH under vigorous stirring. The suspension thus obtained was aged at 60 °C for 8 h, then filtered, washed with distilled water, was finally dried overnight at 80 °C, giving MgAl-LDH solids and the calcined solids were obtained by calcining MgAl-LDH samples at 600 °C for 5 h.

The CuO/MgAl-LDH and MoO_3/MgAl-LDH materials were synthesized by the same method as MgAl-LDH but by adding 5% of CuO or MoO_3 oxides in nitrate salts solution.

The samples were named as follows: MgAl-LDH, 5% CuO/MgAl-LDH, 5%MoO_3/MgAl-LDH and MgAl-LDH-C, 5%CuO/MgAl-LDH-C, 5%MoO_3/MgAl-LDH-C for calcined samples, where the letter C refers to calcined.

Semiconductors photocatalysts characterization

The chemical composition of each solid was established using atomic absorption spectroscopy (AAS) 240FS AA. X-ray diffraction (XRD) patterns were recorded with Siemens D500 diffrcatometer (CuK$\alpha\lambda = 1.54$ Å) at a scanning speed of 2θ/ min from 5 to 80°. Fourier transform infrared (FTIR) spectra were recorded on a Bruker ALPHA spectrophotometer, at a resolution of 2 cm^{-1} and averaging over 20 scans, in the range 400 cm^{-1}–4,000 cm^{-1}. The morphology of the samples were investigated using scanning electron microscopy (Quanta 250) with an accelerating voltage of 20 kV, combined with energy dispersive X-ray spectroscopy (Système EDX Bruker EDS Quantax 200) for the determination of materials composition.

Solar photocatalytic degradation studies

The solar photocatalytic degradation process was conducted in a batch condition using a 500 mL beaker. The MNZ solution with photocatalyst was exposed to sunlight daily

between 11:00 a.m. and 16:00 p.m. while magnetically stirred using a magnetic stirrer.

Prior to irradiation, the solution was magnetically stirred in the dark for 60 min to reach the adsorption-desorption equilibrium. Periodically 5 mL of sample was withdrawn from the beaker and centrifuged (4,000 rpm for 20 min) then the filtrate was analyzed by UV–vis spectrophotometer at 319 nm to determine the residual concentration of MNZ.

The MNZ photodegradation efficiency was calculated as follows:

$$R(\%) = \frac{C_0 - C_i}{C_0} \times 100$$

where C_0 and C_t are the initial concentration and concentration at time (t) of MNZ.

RESULTS AND DISCUSSION

Photocatalysts characterization

The chemical composition of 5%MoO_3/MgAl-LDH-C and 5%CuO/MgAl-LDH-C was determined by atomic absorption spectroscopy (AAS). Table 1 gives the chemical composition and formula of the synthesized materials.

X-ray diffraction (XRD) patterns of the LDH photocatalysts synthesized with addition of CuO and MoO_3 oxides are displayed in Figure 1.

The XRD pattern of both samples 5% CuO/MgAl-LDH and 5% MoO3/MgAl-LDH (Figure 1(A)–1(b) and 1(B)–1(e)) reveals the presence of LDH structure, which is related to the apparition of sharp and symmetric reflections at lower 2Θ value; 2Θ = 11.12 (d_{003}), 2Θ = 22.11 (d_{006}) and 2Θ = 61.22 (d_{110}) (Parida & Mohapatra 2012). At higher 2Θ value a broad and asymmetric peaks are observed, 2Θ = 39 (d_{015}), 2Θ = 47.1 (d_{018}) and 2Θ = 61 (d_{110}). Furthermore, in the XRD pattern of 5% CuO/MgAl-LDH (Figure 1(A)–1(b)) two peaks located at 2Θ = 36 and 39 corresponds to the reflection of CuO are observed (Rat'ko *et al.* 2012). XRD pattern of 5% MoO_3/MgAl-LDH (Figure 1(B)–1(e)) shows two peaks at 2Θ = 25 and 27 corresponds to MoO_3 reflections.

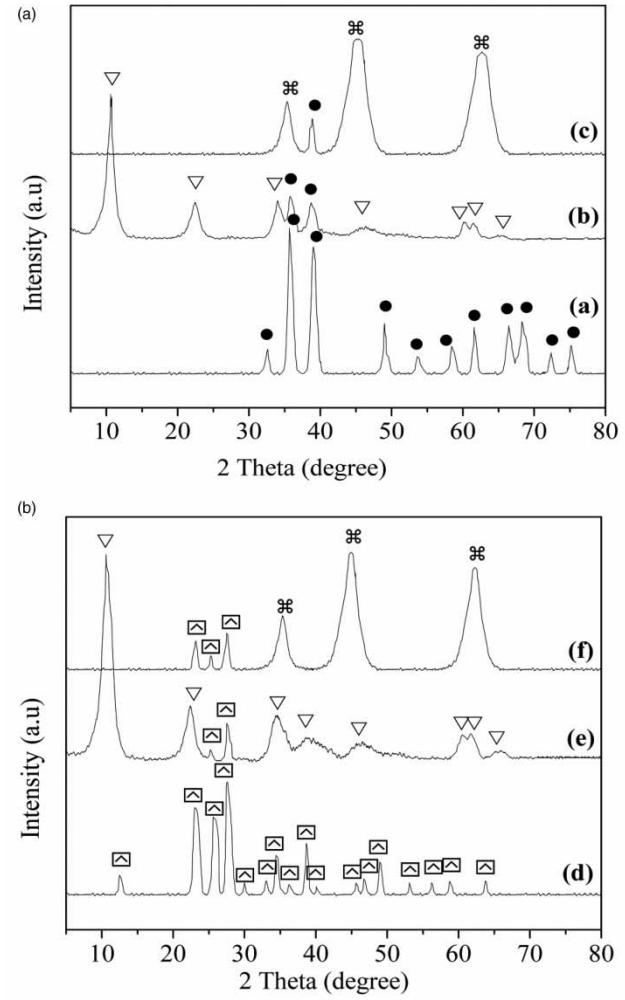

Figure 1 | XRD patterns of the samples: (a) CuO, (b) 5%CuO/MgAl-LDH, (c) 5%CuO/MgAl-LDH-C, (d) MoO_3, (e) 5%MoO_3/MgAl-LDH and (f) 5%MoO_3/MgAl-LDH-C, CuO (●),MoO_3 (▽), LDH (▽) and MgO (⌘).

Upon calcination at 600 °C, we can observe the collapse of LDH structure and formation of oxides metal. The XRD spectra of 5%CuO/MgAl-LDH-C (Figure 1(A)–1(c)) shows peaks related to MgO and CuO, and the spectra of 5% MoO_3/MgAl-LDH-C (Figure 1(B)–1(f)) shows peaks related to MoO_3 and MgO; these results are similar to those previously published elsewhere (Valeikiene *et al.* 2020).

Table 1 | Chemical composition and formula

	Loading (%)						
Solids	**Mg**	**Al**	**Mo**	**Cu**	**Mg^{2+}/Al^{3+} Theoretical**	**$Al^{3+}/(Mg^{2+}+Al^{3+})$**	**Chemical formula**
5%MoO_3/MgAl-LDH-C	17.54	9.29	5.65	–	2	0.35	5%MoO_3/$Mg_{0.65}Al_{0.35}$-LDH-C
5%CuO/MgAl-LDH-C	18.01	7.08	–	5.02	2	0.26	5%CuO/$Mg_{0.74}Al_{0.26}$-LDH-C

The FTIR pattern of synthesized samples is shown in Figure 2. The spectrum shows the typical absorption peaks of carbonate LDH. A broad peak observed at 3,381.72 cm^{-1} for 5%MoO_3/MgAl/LDH sample (Figure 2(a)) and at 3,428.09 cm^{-1} for 5%CuO/MgAl/LDH sample (Figure 2(b)) is related to the hydroxyl stretching vibrations ν(OH).

The sharp absorption peak at about 1,341 cm^{-1} for 5% MoO3/MgAl/LDH sample and at 1,364.9 cm^{-1} for 5% CuO/MgAl/LDH sample can be assigned to the asymmetric stretching mode of the carbonate anions (Jianfeng *et al.* 2015). Finally, the bands ranging from 400 to 800 cm^{-1} can be attributed to the characteristic stretching bands of M-O and O-M-O vibration (He & Zhang 2007; Cheng *et al.* 2010).

As seen from the FTIR spectrum of the calcined samples (Figure 2(c) and 2(d)) all the absorption bands are weakened, compared to the as synthesized LDH, the peak intensity of CO_3^{2-} ions become relatively weaker, indicating that more CO_3^{2-} ions in the interlayer are removed.

The morphology and particle size of synthesized solids were analyzed by TEM and Figure 3 depicts the TEM images. The TEM images of 5%CuO/MgAl-LDH and 5% MoO_3/MgAl-LDH (Figure 3(c) and 3(b)) indicates that the solids show a well-dispersed LDH nanocrystal structure with average particles size in the range of 35–55 nm. While the TEM images of CuO and MoO_3 (Figure 3(a) and 3(d)) shows that the oxides metal CuO and MoO_3 exhibits a core-shell structure.

Photocatalytic studies

The LDH photocatalysts synthesized with addition of CuO and MoO_3 were tested for MNZ solar photocatalysis at the initial MNZ concentration of 10 mg/L for 160 min. As illustrated in Figure 4, the best photocatalysis efficiency was reached with 5%MoO_3/MgAl-LDH-C, the higher efficiency of 5%MoO_3/MgAl-LDH-C was related to the synergistic effects of MoO_3 semiconductor and MgAl-LDH, upon hybridation of these two materials a new semiconductor has been generated with new electric properties.

The photocatalytic performance of 5%MoO_3/MgAl-LDH-C as function of MNZ initial concentration was evaluated by varing the initial MNZ concentration from 10 m/L to 70 mg/L with photocatalyst dose of 1.5 g/L at neutral pH. As shown in Figure 5, the photocatalytic degradation efficiency decreased with increasing the initial MNZ concentration. The photocatalytic efficiency is related to the OH radicals formation on photocatalyst surface. In this case, the weight of photocatalyst is kept constant for each MNZ initial concentration, and the number of OH radicals generated remains constant, while MNZ concentration increases. The ration of OH radicals/MNZ molecules decreases with higher initial MNZ concentration and the probability of MNZ to react with OH radicals decreases, resulting in lower removal efficiency. On the other hand,

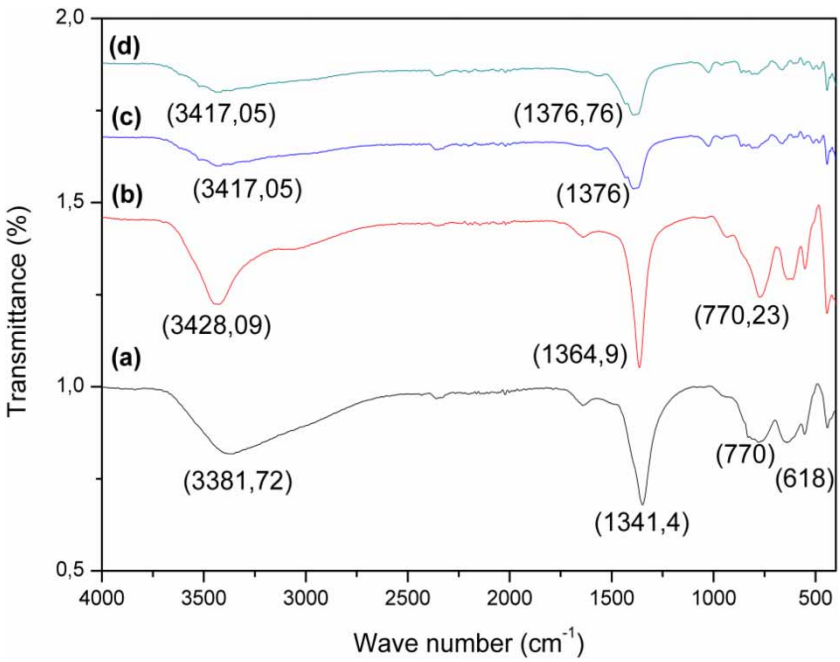

Figure 2 | FTIR spectra of the samples: (a) 5%MoO_3/MgAl-LDH, (b) 5%CuO/MgAl- LDH, (c) 5%MoO_3/MgAl-LDH-C and (d) 5%CuO/MgAl-LDH-C.

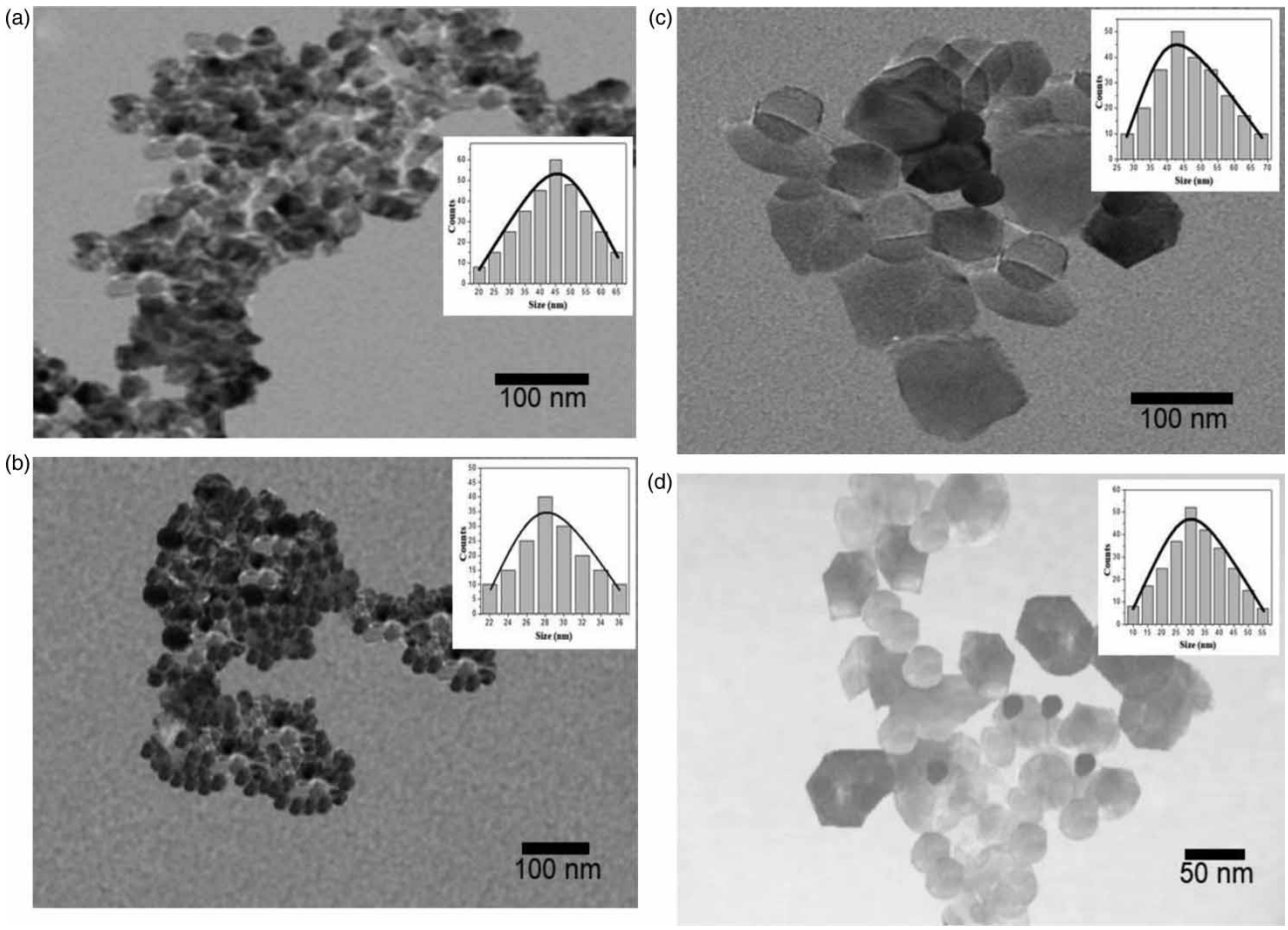

Figure 3 | TEM images of: (a) MoO_3, (b) CuO, (c) 5%MoO_3/MgAl-LDH and (d) 5%CuO/MgAl-LDH.

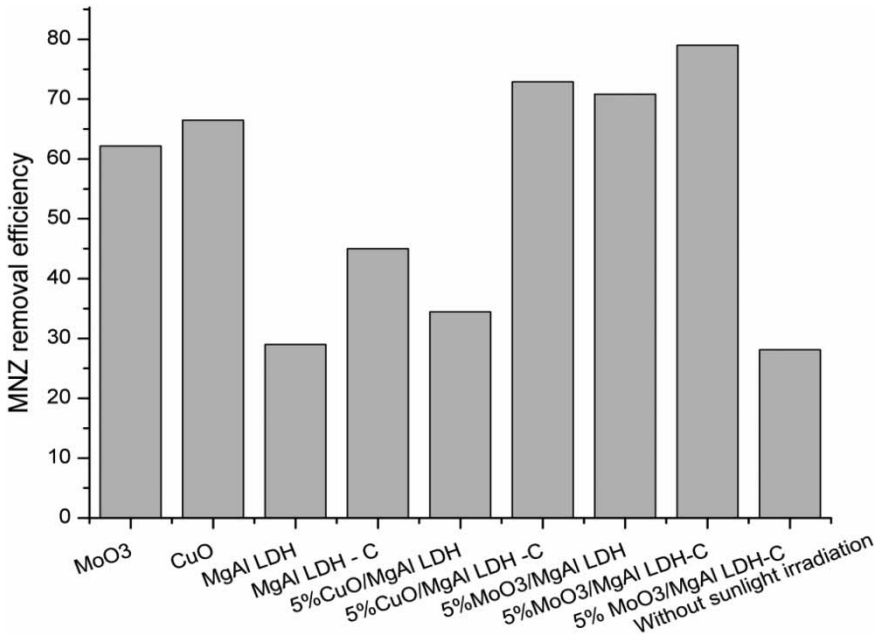

Figure 4 | Comparison between synthesised photocatalysts (photocatalyst dose = 1.5 g/L, C_0 = 10 mg/L, pH = neutral).

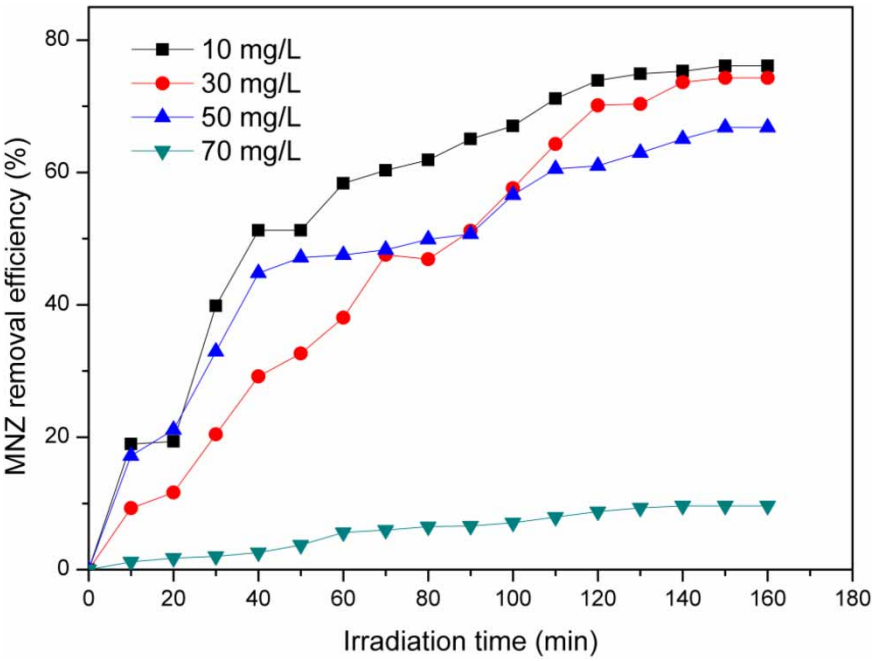

Figure 5 | Effect of initial MNZ concentration on the photocatalysis efficiency of MNZ by 5%MoO_3/Mg Al LDH- C (photocatalyst dose = 1,5 g/L, pH = neutral).

the increasing in MNZ concentration can lead to the decreases of the photon path length that penetrates the pollution solution (Behzad *et al.* 2019).

Figure 6 shows the absorption intensity of MNZ solar photocatalysis using 1.5 g/L of 5%MoO_3/MgAl-LDH-C as photocatalyst, the important change in the peak intensity at 319 nm is observed. Increasing the solar exposure time the absorption intensity decreased.

In order to assess the effect of the photocatalyst dose on the photocatalytic efficiency, the photocatalytic experiments

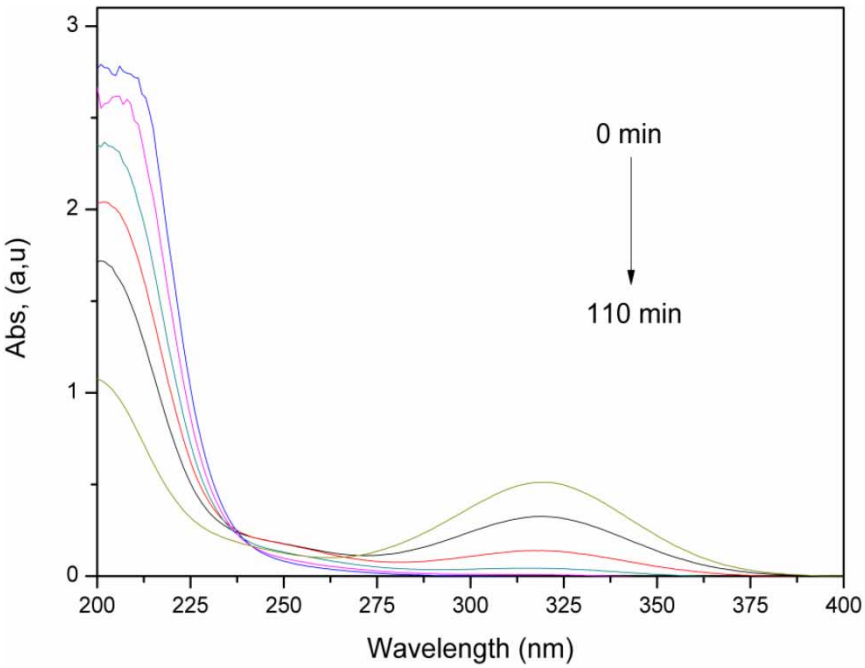

Figure 6 | Evolution of UV-Vis spectra of MNZ with reaction time (initial concentration of MNZ = 10 mg/L, photocatalyst dose = 1.5 g/L at pH = neutral).

with different doses of photocatlyst were conducted. As shown in Figure 7 the increase of photocatalyst dose from 0.5 g/L to 2 g/L improves the photocatalytic degradation efficiency. With increasing the photocatalyst dose, the active sites on the photocatalyst surface will be increased, thus enhancing the photons absorbed by the photocatalyst causing the enhancement of photocatalytic efficiency. Therefore, the optimum photocatalyst dose was fixed as 1.5 g/L for the next studies.

By further increasing the photocatalyst dose until 2 g/L, high penetration may partly be impeded due to screening effects, thus reducing degradation efficiency (Behzad *et al.* 2019).

Kinetics of MNZ solar photocatalytic degradation

The reaction kinetic of MNZ removal by 5%MoO_3/MgAl-LDH-C was investigated using the Langmuir–Hinshelwood model.

The model expression can be represented by the first-order kinetic as given below:

$$r = -\frac{dc}{dt} = \frac{K_r K_{ad} C}{1 + K_{ad} C}$$

where k_r is the intrinsic rate constant and K_{ad} is the adsorption equilibrium constant. At low initial organic pollutant concentration K_{ad} C is negligible and the model equation becomes as follows:

$$r = -\frac{dc}{dt} = K_r K_{ad} C$$

After integration the Langmuir–Hinshelwood model is given as:

$$\ln \frac{C_0}{C} = K_{app} t$$

where C_0 is the initial organic pollutant concentration at adsorption–desorption equilibrium a $t = 0$ min and K_{app} is the apparent rate constant ($K_{app} = Kr\ K_{ad}$).

The half-life time ($t_{1/2}$) of the photodegradation process is given as:

$$t_{1/2} = \frac{\ln (2)}{K_{app}}$$

The apparent rate constant K_{app} and R^2 were calculated from the linear plot ln (C_0/C) versus irradiation time (t) as shown in Figure 8 and the obtained results are illustrated in Table 2.

MNZ photocatalytic degradation results well-fitted the pseudo-first-order kinetic model, with coefficients (R^2)

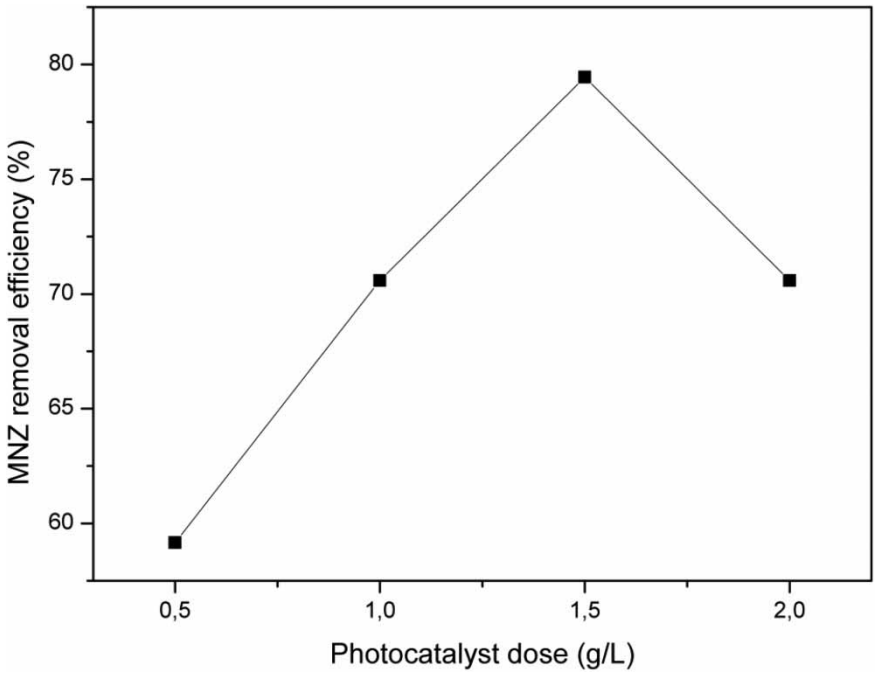

Figure 7 | Effect of photocatalyst dose on the photodegradation efficiency of MNZ by 5%MoO_3/Mg Al- LDH-C ($C_0 = 10$ mg/L, pH = neutral).

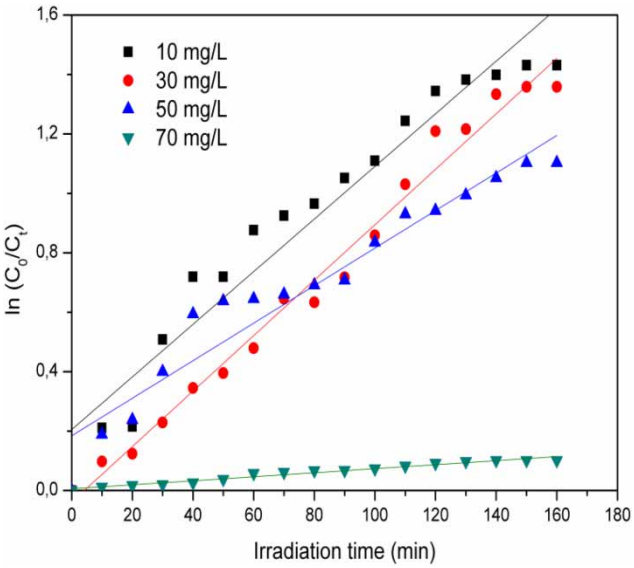

Figure 8 | Pseudo-first-order kinetics photodegradation of MNZ, by Langmuir–Hinshelwood model onto 5%MoO_3/Mg Al LDH- C (photocatalyst dose = 1.5 g/L, pH = neutral).

Table 2 | Langmuir–Hinshelwood model parameters of photocatalysis degradation

MNZ Initial concentration (mg/)	K_{app}* 10^{-2}	$t_{1/2}$	R^2
10	0.886	78.21	0.936
30	0.933	74.27	0.983
50	0.632	109.65	0.933
70	0.064	1,034.13	0.965

more than 0.93. Increasing the MNZ initial concentration the apparent rate decreased, this result is related to the decreases in the hydroxyl radical generated, when increasing the MNZ initial concentration the solar light photons will be adsorbed by MNZ molecules rather than the photocatalyst (Collazzo *et al.* 2012; Kalebaila & Fairbridge 2014).

Table 3 illustrates the photocatalytic MNZ degradation studies published in the literature. When comparing these photocatalytic MNZ degradation studies with our study, it can be seen that these works use artificial radiation, making the process expensive. In our work, we tested higher concentration of MNZ (10, 30, 50 and 70 mg/L), and used inexpensive sunlight radiation. The utilization of solar-light as a promoter in the field of molecular photodegradation can provide many advantages such as eliminating the use of energy-demanding UV-lamps, which are usually made of toxic mercury. Several studies have reported about MNZ photocatalytic degradation. However, few of them focus on the solar radiation.

Photocatalytic degradation mechanism of MNZ

The reaction mechanism of MNZ removal by MoO_3-alone, CuO-alone, 5%MoO_3/MgAl LDH-C, 5%MoO_3/MgAl-LDH, 5%CuO/MgAl-LDH-C and 5%CuO/MgAl-LDH could be proposed as following (Equations (1)–(10)). An electron (e^-) of a semiconductor (A) excites from the valence band to the conduction band, creating an electron–hole (h+) couple (Reaction (1)) (Elmolla & Chaudhuri 2010; Farzadkia *et al.* 2015). The generated electron–hole pairs react with either electron acceptors like O_2 and donors like H_2O or OH^- adsorbed on the semiconductor surface to generate strong reactive radical species (Reactions (2) and (3)). Then, positive holes can oxidize pollutants directly, too (Reaction (4)) (Elmolla & Chaudhuri 2010; Farzadkia *et al.* 2015).

$$A + h\gamma \rightarrow A(e^- + h^+) \quad \text{(Reaction 1)}$$

$$h^+ + H_2O \rightarrow h^+ + \cdot OH \quad \text{(Reaction 2)}$$

$$h^+ + OH^- \rightarrow \cdot OH \quad \text{(Reaction 3)}$$

$$MNZ + \cdot OH \rightarrow Degradation\ Products \quad \text{(Reaction 4)}$$

when oxygen is present in the CB can generate a super-peroxide anion which can produce organic peroxide and hydrogen peroxide (Reactions (5)–(8)).

$$O_2 + e^- \rightarrow \cdot O_2^- \quad \text{(Reaction 5)}$$

$$\cdot O_2^- + H^+ \rightarrow HO_2^{\cdot} \quad \text{(Reaction 6)}$$

$$HO_2^{\cdot} + HO_2^{\cdot} \rightarrow H_2O_2 + O_2 \quad \text{(Reaction 7)}$$

$$H_2O_2 + e^- \rightarrow OH^- + \cdot OH \quad \text{(Reaction 8)}$$

$$H_2O_2 + \cdot O_2^- \rightarrow OH^- + \cdot OH + O_2 \quad \text{(Reaction 9)}$$

Reusability of MoO_3/MgAl-LDH-C phtocatalyst

The reusability of MoO_3/MgAl-LDH-C (1.5 g/L) catalyst in the photodegradation of MNZ (C_{MNZ} = 10 mg/L) at free pH was also studied under sunlight conditions over the course of 60 min. Figure 9 shows the results of the reusability test of MoO_3/MgAl-LDH-C photocatalyst for the photocatalytic degradation of MNZ within four successive cycles. The photocatalyst in any run was collected, washed with distilled water, dried and then used in a new experiment. It could be observed that the degradation efficiency of MNZ was decreased slightly after five repeated

Table 3 | MNZ photocatalytic degradation studies published in the literature

Photocatalyst	Dose (g/L)	MNZ initial Concentration (mg/L)	Experimental condition	Rate of degradation	Reference
Copper oxide nanoparticles	0.2	1	15 W UV-254 lamp mercury	85% 120 min radiation	Khataee *et al.* (2013)
Immobilization of TiO_2 on ceramic plates	–	10	Three 30-W (UV–C lamps Philips)	95.32% 150 min radiation	El-Sayed *et al.* (2014)
Phosphorus-doped g-C_3N4/Co_3O_4q	1	10	Visible light irradiation (250 W Xelamp)	80% 180 min radiation	Zhao *et al.* (2019)
5%MoO_3/MgAl-LDH-C	1.5	10	Solar light radiation	80% 60 min solar light	This study

(Khataee *et al.* 2013; El-Sayed *et al.* 2014; Zhao *et al.* 2019).

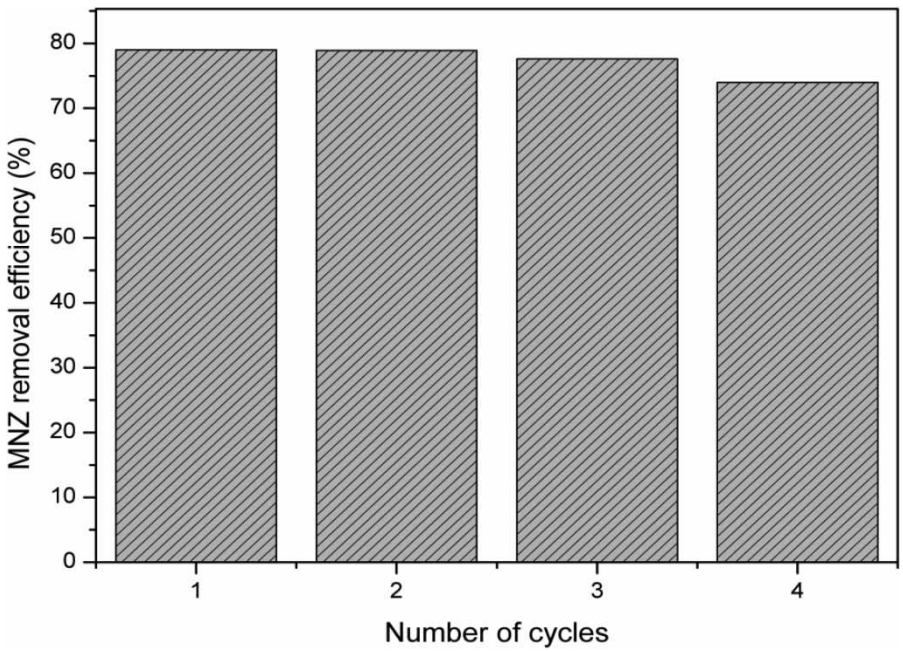

Figure 9 | Reusability of the MoO_3/MgAl-LDH-C within four consecutive experimental runs ($C_0 = 10$ mg/L, photocatalyst dose = 1.5 g/L, pH = neutral).

experimental runs, thereby indicating that the as-prepared MoO_3/MgAl-LDH-C could be used as a promising photocatalyst for the degradation of organic pollutants with a significant reusability potential.

CONCLUSION

The hybrid semiconductors MnO_3, CuO, uncalcined and calcined MgAl-LDH have been successfully synthesized by co-precipitation method and tested for MNZ removal by solar photocatalysis process. The 5%MnO_3/MgAl-LDH-C solid is very promising photocatalyst for the removal of organic pollutants for wastewater using photocatalysis method under solar irradiation, since the solar irradiation is an environmentally friendly light source, the MNZ solution is used at pH neutral without adjustment and the photocatalysis is realised without addition of scavengers.

DATA AVAILABILITY STATEMENT

All relevant data are included in the paper or its Supplementary Information.

REFERENCES

Ahmadpour, N., Sayadi, M. H., Sobhani, S. & Hajiani, M. 2020 Photocatalytic degradation of model pharmaceutical pollutant by novel magnetic TiO_2@$ZnFe_2O_4$/Pd nanocomposite with enhanced photocatalytic activity and

stability under solar light irradiation. *Journal of Environmental Management* **271**, 110964.

Behzad, S., Farzaneh, F., Shadi, K., Afshin, M., Mohammadamin, P., Yahya, Z., Yuxuan, G., Jixiang, Y., Gordon, M., Seung-Mok, L. & Jae-Kyu, Y. 2019 Application of cadmium doped ZnO for the solar photocatalytic degradation of phenol. *Water Science and Technology* **79** (2), 375–385.

Cheng, X., Huang, X., Wang, X. & Sun, D. 2010 Influence of calcination on the adsorptive removal of phosphate by Zn–Al layered double hydroxides from excess sludge liquor. *Journal of Hazardous Materials* **177**, 516–523.

Collazzo, G. C., Jahn, S. L. & Foletto, E. L. 2012 Removal of direct black 38 dye by adsorption and photocatalytic degradation on TiO_2 prepared at low temperature. *Latin American Applied Research* **42**, 55–60.

Czech, B., Zygmunt, P., Kadirova, Z. C., Yubuta, K. & Hojamberdiev, M. 2020 Effective photocatalytic removal of selected pharmaceuticals and personal care products by elsmoreite/tungsten oxide@ZnS photocatalyst. *Journal of Environmental Management* **270**, 110870.

Elmolla, E. S. & Chaudhuri, M. 2010 Photocatalytic degradation of amoxicillin, ampicillin and cloxacillin antibiotics in aqueous solution using UV/TiO_2 and UV/H_2O_2/TiO_2 photocatalysis. *Desalination* **252**, 46–52.

El-Sayed, G., Dessouki, H., Jahin, H. & Ibrahiem, S. 2014 Photocatalytic degradation of metronidazole in aqueous solutions by copper oxide nanoparticles. *Journal of Basic and Environmental Sciences* **1**, 1102–1110.

Fagan, R., McCormack, D. E., Dionysiou, D. D. & Pillai, S. C. 2016 A review of solar and visible light active TiO_2 photocatalysis for treating bacteria, cyanotoxins and contaminants of emerging concern. *Materials Science in Semiconductor Processing* **42**, 2–14.

Farzadkia, M., Bazrafshan, E., Esrafili, A., Yang, J. K. & Shirzad-Siboni, M. 2015 Photocatalytic degradation of metronidazole with illuminated TiO_2 nanoparticles. *Journal of Environmental Health Science & Engineering* **13**, 35.

He, F. A. & Zhang, L. M. 2007 New polyethylene nanocomposites prepared by in-situ polymerization method using nickel a-diimine catalyst supported on organo modifified ZnAl layered double hydroxide. *Composites Science Technology* **67**, 3226–3232.

He, K., Li, M. & Guo, L. 2012 Preparation and photocatalytic activity of PANI-CdS compo-sites for hydrogen evolution. *International Journal of Hydrogen Energy* **37**, 755–759.

Jianfeng, M., Jiafan, D., Liangmin, Y., Liangyin, L., Yong, K. & Sridhar, K. 2015 Synthesis of Fe_2O_3–NiO–Cr_2O_3 composites from NiFe-layered double hydroxide for degrading methylene blue under visible light. *Applied Clay Science* **107**, 85–89.

Kalebaila, K. K. & Fairbridge, C. 2014 UV photocatalytic degradation of commercial naphthenic acid using TiO_2-zeolite composites. *Journal of Water Resource and Protection* **6** (12), 1198–1206.

Kanakaraju, D., Glass, B. D. & Oelgemöller, M. 2018 Advanced oxidation process-mediated removal of pharmaceuticals from water: a review. *Journal of Environmental Management* **219**, 189–207.

Khataee, A. R., Fathinia, M. & Joo, S. W. 2013 Simultaneous monitoring of photocatalysis of three pharmaceuticals byimmobilized TiO_2 nanoparticles: chemometric assessment, intermediates identification and ecotoxicological evaluation. *Spectrochim Acta A: Molecular and Biomolecular Spectroscopy* **112**, 33–45.

Kim, S. P., Choi, M. Y. & Choi, H. C. 2016 Photocatalytic activity of sno_2 nanoparticles in methylene blue degradation. *Materials Research Bulletin* **74**, 85–89.

Mecha, A., Onyango, C., Ochieng, M. S., Jamil, A., Fourie, T. S., & Momba, C. J. S. & B, M. N. 2016 UV and solar light photocatalytic removal of organic contaminants in municipal wastewater. *Separation Science and Technology* **51**, 10.

Nguyen, D. T., Tran, H. N., Juang, R. S., Dat, N. D., Tomul, F., Ivanets, A., Woo, S. H., Bandegharaei, A. H., Nguyen, V. P. & Chao, H. P. 2020 Adsorption process and mechanism of Acetaminophen onto commercial activated carbon. *Journal of Environmental Chemical Engineering* **8** (6), 104408.

Parida, K. M. & Mohapatra, L. 2012 Carbonate intercalated Zn/Fe layered double hydroxide: a novel photocatalyst for the enhanced photodegradation of azo dyes. *Chemical Engineering Journal* **179**, 131–139.

Pereira, J. M., Calisto, V. & Santos, S. M. 2019 Computational optimization of bioadsorbents for the removal of pharmaceuticals from water. *Journal of Molecular Liquids* **279**, 669–676.

Pichat, P., Vannier, S., Dussaud, J. & Rubis, J. P. 2005 Assessment of solar photocatalysis to purify on-site rinse waters from tractor cisterns used in grapevine pest control: field experimentation. *Water Science and Technology* **52** (8), 223–230.

Prasad, C., Tang, H., Liu, Q. Q., Zulfiqar, S., Shah, S. & Bahadur, I. 2019 An overview of semiconductors/layered double hydroxides composites: properties, synthesis, photocatalytic and photoelectrochemical applications. *Journal of Molecular Liquids* **289**, 111114.

Rat'ko, A. I., Ivanets, A. I. & Voronet, E. A. 2012 Copper-Magnesium oxide catalyst based on modified dolomite. *Russian Journal of Applied Chemistry* **85** (6), 856–861.

Valeikiene, L., Roshchina, M., Puroniene, I. G., Prozorovich, V., Zarkov, A., Ivanets, A. & Kareiva, A. 2020 On the reconstruction peculiarities of sol–gel derived Mg2 – xMx/Al1 (M = Ca, Sr, Ba) layered double hydroxides. *Crystals* **10**, 470.

Zhang, X., Wang, Y., Hou, F., Li, H., Yang, Y., Zhang, X., Yang, Y. & Wang, Y. 2017 Effects of Ag loading on structural and photocatalytic properties off lower-like ZnO microspheres. *Applied Surface Science* **391**, 476–483.

Zhao, Y., Hu, W., Chen, J. & Lv, L. 2012 Factors influencing the chloride removal of aqueous solution by calcined layered double hydroxides. *Desalination and Water Treatment* **36**, 50–56.

Zhao, Z., Fan, J., Deng, X. & Liu, J. 2019 One-step synthesis of phosphorus-doped g-C_3N_4/Co_3O_4 quantum dots from vitamin B12 with enhanced visible-light photocatalytic activity for metronidazole degradation. *Chemical Engineering Journal* **360**, 1517–1529.

First received 16 August 2020; accepted in revised form 19 October 2020. Available online 30 October 2020